Polyhedron 232 (2023) 116275

Contents lists available at ScienceDirect

Polyhedron

journal homepage: www.elsevier.com/locate/poly

A pentagonal bipyramidal Co(II) single-ion magnet based on an asymmetric tetradentate ligand with easy plane anisotropy

Xing-Cai Huang [a,c,*], Wei Yong [a], Shruti Moorthy [b], Zhang-Yu Su [a], Jiao-Jiao Kong [a], Saurabh Kumar Singh [b,*]

[a] School of Chemistry and Environmental Engineering, Yancheng Teachers University, Yancheng 224007, China
[b] Department of Chemistry, Indian Institute of Technology Hyderabad, Kandi-502285, Sangareddy, Telangana, India
[c] State Key Laboratory of Coordination Chemistry, Nanjing University, Nanjing 210093, China

ARTICLE INFO

Keywords:
Co(II)
Single-ion magnet
Easy plane anisotropy
Pentagonal bipyramid
Theoretical calculations

ABSTRACT

High-coordinate 3d single-ion magnets(SIMs) especially with pentagonal bipyramidal geometry as an emerging class of representative molecular magnets have received considerable concern. Whereas, it is not easy to construct and obtain 3d SIMs with high coordination numbers (CN = 7 or 8). Herein, a mononuclear Co(II) complex ([Co(pypzbeyz)$(NCS)_2$(DMF)], pypzbeyz = N-((6-(1H-pyrazol-1-yl)pyridin-2-yl)methylene)benzohydrazide) based on a tetradentate ligand has been synthesized and structurally and magnetically characterized. Single-crystal X-ray diffraction analysis reveals that the Co(II) complex adopts a seven-coordinate distorted pentagonal bipyramidal geometry. Magnetic investigations show that the Co(II) complex has large easy plane anisotropy with a positive D value (D = +36.8 cm^{-1}) and a small E value, and exhibits slow magnetic relaxation behavior under a dc field. Theoretical calculations show a positive zero-field splitting of 33.5 cm^{-1}, which is in excellent agreement with the experiment. The results support that the 3d high-coordinate SIMs could be effectively achieved by using a suitable multi-dentate ligand with a certain ligand field.

1. Introduction

Mononuclear single-molecule magnets (also called single-ion magnets (SIMs)) have attracted great attention due to their promising applications in information storage [1–3] and spintronic devices [4,5]. Since the first discovery of Fe(II) SIM [6], the 3d SIMs have sprung up for their unique advantages of tuning and manipulating magnetic anisotropy. Till now, the two-coordinate [Co(C$(SiMe_2Ph)_3)_2$] has reached the highest spin relaxation barrier of 450 cm^{-1} [7]. The orbital angular momentum leads to magnetic anisotropy which can be quenched by the ligand field. To gain high performance for 3d SIMs, the 3d complexes with unquenched orbital angular momentum in a specific coordination geometry can give rise to large magnetic anisotropy. Generally, the magnetic anisotropy can be determined by the zero-field splitting parameters D and E. The negative and positive D values represent easy-axis anisotropy and easy-plane anisotropy, respectively. From a synthetic point of view, it can be designed by utilizing different chelating ligands to obtain the specific symmetry group. Furthermore, the 3d complexes with low coordination numbers (CN = 2–5) favor bulky ligands with steric interactions, and the ligands with high chelating atoms (>4) for Kramers Co(II) ion usually prefer high coordination numbers (CN = 7, 8). Although the effective energy barrier of high-coordinate 3d SIMs is not as high as the low-coordinate ones, the high-coordinate 3d SIMs also provide another practical solution for pursuing the structure–activity relationship for the 3d SIMs. Remarkably, the ligand design strategy can make full use of the ligand-field theory to develop high-coordinate 3d SIMs. Arranging many alternative chelating atoms in the specific ligand supplies the weak ligand field for constructing high-spin 3d metal complexes, which can possess slow magnetic relaxation behavior.

From the first discovery of SIM [(3G)CoCl](CF_3SO_3) (3G = 1, 1, 1-tris-[2 N-(1,1,3,3-tetramethylguanidino)methyl]ethane) with positive D value [8], the reported 3d complexes showed slow magnetic relaxation behaviour with positive D value (easy-plane anisotropy), which can be adapted the trigonal planar (CN = 3, D_{3h}) [9], tetrahedral (CN = 4, T_d) [10,11], square pyramidal (CN = 5, C_{4v}) [12], trigonal pyramidal (CN = 5, D_{3h}) [13], octahedral (CN = 6, O_h) [14–16], pentagonal bipyramidal (CN = 7, D_{5h}) [17–20], capped trigonal prism (CN = 7, C_{2v}), [21] and other coordination geometry. It should be pointed out that the easy

* Corresponding authors at: School of Chemistry and Environmental Engineering, Yancheng Teachers University, Yancheng 224007, China (X.-C. Huang).
E-mail addresses: huangxc82@126.com (X.-C. Huang), sksingh@chy.iith.ac.in (S.K. Singh).

https://doi.org/10.1016/j.poly.2022.116275
Received 5 November 2022; Accepted 25 December 2022
Available online 30 December 2022

plane magnetic anisotropy (the positive value) can occur for Kramers Co (II) ions with a high CN = 7. To obtain the 3d SIMs with high coordination numbers, the tetradentate and pentadentate ligands as the favorable ligands were utilized to construct the suitable ligand field. We have successfully reported the seven-coordinate Co(II) SIMs with positive *D* values based on the pentadentate ligands [17], a tetradentate ligand [22], and a bidentate ligand [21]. It is vital to figure out the relationship between the magnetic properties and structure for predicting and designing the new 3d SIMs with high coordination numbers. Additionally, the investigation of novel high-coordinate 3d SIMs with easy-plane magnetic anisotropy could promote other approaches to obtaining high-performance SMMs for practical application.

Inspired by this consideration, we further aim to gain the high-coordinate 3d SIMs with pentagonal bipyramid(D_{5h}) to understand the relationship between the magnetic properties and structure. The asymmetric tetradentate ligand pypzbeyz could tend to obtain high-coordinate 3d complexes. Herein, a mononuclear Co(II) complex ([Co(pypzbeyz)$(NCS)_2$(DMF)]) based on the tetradentate ligand has been reported. X-ray crystal structure analysis revealed that the Co(II) complex is a seven-coordinate complex with distorted pentagonal bipyramidal geometry (D_{5h}). Magnetic susceptibilities studies revealed that the Co(II) complex possessed relatively large easy-plane anisotropy ($D > 0$), and showed slow magnetic relaxation behavior under a dc field. Theoretical calculations gave detailed results to identify the experiment results for the pentagonal bipyramidal Co(II) complex with easy plane anisotropy. The results could pave the way to design and construct high-coordinate 3d SIMs based on the tetradentate ligands.

2. Materials and methods

2.1. Materials

All preparations and manipulations were performed under aerobic conditions. The ligand N-((6-(1H-pyrazol-1-yl)pyridin-2-yl)methylene) benzohydrazide (pypzbeyz) was prepared according to our previous work [22].

2.2. Synthesis of 1 ([Co(pypzbeyz)$(NCS)_2$(DMF)])

To a solution of pypzbeyz (0.10 mmol, 29.1 mg), $Co(NCS)_2$ (0.10 mmol, 17.5 mg) in a 5 mL mixed solution of CH_3OH and DMF(V_{CH3OH}/V_{DMF} = 1:1). The mixture was tackled by ultrasonic vibration for 5 min to yield the dark green solution and then filtered. The pale orange block crystals suitable for X-ray diffraction studies were obtained by slow diffusion of diethyl ether vapor into the resulting solution after 2 days. Yield: ca. 35 %. Elemental analysis (%) calculated for $C_{21}H_{20}N_8O_2S_2Co$: C, 46.75 %; H, 3.74 %; N, 20.77 %. Found: C, 46.34; H, 3.82; N, 20.89. IR (KBr, cm^{-1}): 3447(w), 3100(m), 3029(m), 2964(w), 2935(w), 2798(w), 2122(s), 2095(vs), 1647(vs), 1616(w), 1602(w), 1572(s), 1530(s), 1478 (s), 1463(m), 1448(w), 1400(m), 1375(m), 1365(m), 1344(w), 1296(s), 1276(s), 1227(w), 1205(w), 1176(m), 1145(m), 1105(m), 1099(s), 1069(w), 1049(m), 1028(w), 1008(w), 975(m), 928(m), 912(w), 885 (w), 796(m), 762(m), 731(w), 710(m), 687(m), 679(s), 650 (w), 628 (w), 626(w), 597(w), 532(w), 471(w).

2.3. Physical measurements

Elemental analyses for C, H and N were carried out a Vario EL II Elementar. Infrared spectra were performed on a VERTE 80 spectrometer with pressed KBr pellets in the range 400–4000 cm^{-1} at room temperature. Magnetic measurements were carried on a Quantum Design SQUID VSM magnetometer at temperatures ranging from 1.8 K to 300 K for dc fields ranging from 0 to 7 T with the ground crystalline samples. All data were corrected for the diamagnetism contribution of the sample holder and the complex using Pascal's constants [23].

2.4. X-ray data collection, structure solution and refinement

The X-ray data of **1** were collected on a Bruker D8 QUEST diffractometer equipped with a CMOS area detector of Mo-Kα radiation (λ = 0.71073 Å). The APEX III program was used to determine the unit cell parameters and for data collection. The data were integrated using SAINT [24] and SADABS 2016/2 [25]. The structures for both two complexes were solved by direct methods and refined by full-matrix least-squares based on F^2 using the SHELXL-2014/7 package [26]. All the non-hydrogen atoms were refined anisotropically. Hydrogen atoms of the organic ligands were refined as riding on the corresponding non-hydrogen atoms. Additional details of the data collection and structural refinement parameters are provided in Table 1. Selected bond lengths and angles are listed in Table 2.

2.5. Computational details

All calculations were carried out on ORCA 4.2.1 code [27]. The position of hydrogens were optimized using BP86 [28,29] level of theory and def2-SVP [30] for all atoms. Further calculations were carried out on the hydrogen optimized coordinates. For the calculation of spin-Hamiltonian parameters and the electronic, magnetic properties, we used DKH-def2-TZVPP [30] for Cobalt and DKH-def2-SVP [30] for all other atoms. Complete active space self-consistent (CASSCF) [31] method was used with an active space of seven electrons in five d-orbitals, CAS(7,5). Using this active space, we computed 10 quartet states and 40 doublet states. On the converged CASSCF wavefunction, second-order *N*-electron valence perturbation theory (NEVPT2) [32–34] method was employed to account for the dynamic correlations. Further, ab-initio based ligand field theory (AILFT) analysis was used for the analysis of ligand field and d-orbital splitting as implemented in ORCA.

Table 1
Crystallographic data and structure refinement for **1**.

complex	**1**
Formula	$C_{21}H_{20}N_8O_2S_2Co$
*M*r [g mol^{-1}]	539.50
CCDC number	2217639
Crystal size[mm^3]	0.42 × 0.36 × 0.28
Crystal system	Triclinic
Space group	$P\bar{1}$
a [Å]	7.356(3)
b [Å]	13.099(2)
c [Å]	13.295(4)
α [°]	74.271(5)
β [°]	79.952(7)
γ [°]	77.324(6)
V [Å^3]	1193.9(6)
Z	2
T, K	293(2)
ρ_{calcd} [g cm^{-3}]	1.501
μ(Mo–*K*α) [mm^{-1}]	0.930
F (0 0 0)	554
θ range [°]	2.860–27.541
Refl. collected/unique	21,311/5492
R(int)	0.0235
T_{max}/T_{min}	0.5214/0.3997
Data/restraints/parameters	5492/0/313
R_1[a]/wR_2[b]($I > 2\sigma(I)$)	0.0299/0.0762
R_1/wR_2 (all data)	0.0377/0.0801
GOF on F^2	1.040
Max/min [e Å^{-3}]	0.381/−0.336

[a] $R_1 = \sum||F_o| - |F_c||/\sum|F_o|$.
[b] $wR_2 = \{\sum[w(F_o^2 vF_c^2)^2]/\sum[w(F_o^2)^2]\}^{1/2}$.

Table 2
Selected Bond Distances [Å] and angles [°] for **1** and **2**.

1			
Co(1)–N(6)	2.071(3)	Co(1)–N(3)	2.248(3)
Co(1)–N(7)	2.085(3)	Co(1)–N(4)	2.269(3)
Co(1)–O(2)	2.181(3)	Co(1)–O(1)	2.280(3)
Co(1)–N(1)	2.241(3)		
N(6)–Co(1)–N(7)	177.24(6)	N(7)–Co(1)–N(1)	87.83(7)
N(6)–Co(1)–O(2)	86.95(8)	O(2)–Co(1)–N(1)	146.69(6)
N(7)–Co(1)–O(2)	91.19(8)	N(6)–Co(1)–N(3)	91.12(11)
N(6)–Co(1)–N(1)	94.84(7)	N(7)–Co(1)–N(3)	90.43(11)
O(2)–Co(1)–N(3)	76.61(11)	O(2)–Co(1)–N(4)	144.56(6)
N(1)–Co(1)–N(3)	70.10(8)	N(1)–Co(1)–N(4)	68.59(6)
N(6)–Co(1)–N(4)	85.80(11)	N(3)–Co(1)–N(4)	138.13(9)
N(7)–Co(1)–N(4)	94.56(11)	N(6)–Co(1)–O(1)	87.84(9)
N(7)–Co(1)–O(1)	89.75(10)	N(3)–Co(1)–O(1)	153.58(5)
O(2)–Co(1)–O(1)	76.97(11)	N(4)–Co(1)–O(1)	68.13(9)
N(1)–Co(1)–O(1)	136.30(8)		

3. Results and discussion

3.1. Description of crystal structures 1.

X-ray single-crystal diffraction results reveal that **1** crystallizes in the $P\bar{1}$ space group of a triclinic system (Table 1). Complex **1** consists of a Co (II) ion, one asymmetric tetradentate ligand **pypzbeyz**, two coordinated NCS^- and one coordinated DMF molecule (Fig. 1a). In complex **1**, the Co (II) center adopts a hepta-coordinate (N_5O_2) ligand set with a distorted pentagonal bipyramidal geometry (D_{5h} symmetry)(Fig. 1b). In the coordination polyhedron of complex **1**, five N_3O_2 atoms from **pypzbeyz** (N1, N3, N4, O1) and one DMF (O2) occupied the equatorial plane five positions, and the axial two positions are occupied by two N_2 atoms from NCS^-(N6 and N7). As shown in Table 2, the bond angle of ∠N6-Co1-N7 is 177.24(6)° almost close to the ideal 180°, and the bond angles in the pentagon of the coordination polyhedron range from 68.13(9)°(∠N4-Co1-O1) to 76.97(11)°(∠O1-Co1-O2), which are deviated from the ideal 72°. Therefore, the distorted degree can be calculated by the continuous shape measures (CShM) software SHAPE 2.1 [35] to yield the value of 0.428(0 means ideal pentagonal bipyramidal geometry, Table S1). The supramolecular interactions (π-π stackings) between two neighbour complexes were found between the neighbour benzene rings in the ligand **pypzbeyz** with 3.741(6) and 3.665(6) Å (Fig. 1c), but no classic hydrogen bond was found. In addition, the shortest Co1···Co1 distance is 7.356(1) Å (Fig. 1c), which can be neglected the magnetic interaction between Co1 atoms in the solid state.

3.2. Magnetic properties of complex 1

The dc magnetic susceptibilities of complex **1** were determined on polycrystalline samples in the temperature range of 300 –1.8 K under a 1000 Oe dc field (Fig. 2a). The $\chi_M T$ value at 300 K is 2.66 cm^3 mol^{-1} K

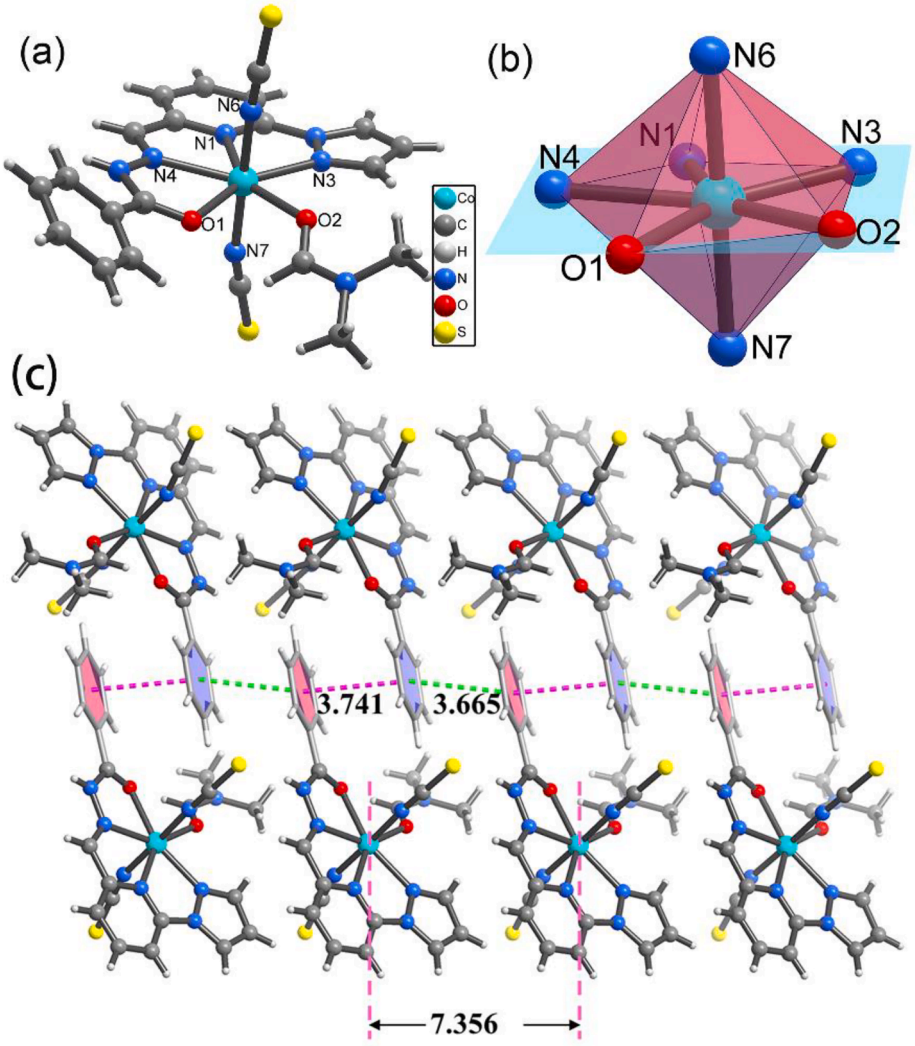

Fig. 1. Crystal structure of complex **1**(a), the coordination polyhedron around Co(II) (b), and π-π stackings distances and the shortest Co1···Co1 distance(c).

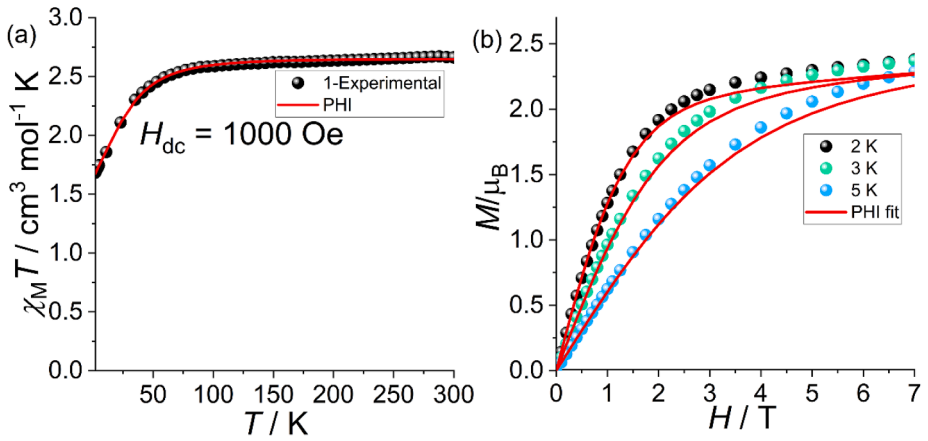

Fig. 2. (a) Temperature dependence of χ_MT products for complex **1** under a dc field of 1000 Oe. (b) Field dependence of the magnetization data at 2, 3, and 5 K for **1**. The red solid lines are fitted simultaneously by using PHI software.

for **1**, which are larger than the theoretical values of 1.875 cm^3 mol^{-1} K for the spin-only high-spin Co(II) ion ($S = 3/2$, $g_{Co} = 2.0$), indicating the high-spin Co(II) ion with a distorted pentagonal bipyramidal geometry processing the high magnetic anisotropy. Upon lowering the temperature, the χ_MT for **1** gradually decreases and then drops to reach 1.68 cm^3 mol^{-1} K at 2.0 K. The χ_MT curves are similar to the most reported mononuclear Co(II) SIMs. The magnetization of **1** at 2, 3, and 5 K increases up to 2.38, 2.37, and 2.29 μ_B at 7 T (Fig. 2b), respectively, which is lower than the calculated saturation value(3.0 μ_B), further identifying the significant magnetic anisotropy of Co(II) in complex **1**.

To gain insight into the magnetic anisotropy of Co(II) in **1**, the simultaneously fit for the magnetic susceptibilities and magnetization at 2, 3, and 5 K(Fig. 2) by using the PHI software [36] gave the ZFS parameters according to the spin Hamiltonian equation $H = D[\hat{S}_z^2 - S(S+1)/3] + E(\hat{S}_x^2 - \hat{S}_y^2) + \mu_B (g_x\hat{S}_xB_x + g_y\hat{S}_yB_y + g_z\hat{S}_yB_z)$ where D, E, S_i, g_i, B_i, and μ_B represent for the uniaxial ZFS parameter, transverse ZFS parameter, spin operator, g tensor, magnetic vector, and Bohr magneton, respectively. The fit curves with different temperatures for complex **1** are not totally consistent with the M vs H plots, due to the highly anisotropic feature of the Co(II) center. The best fit afforded D = 36.8 cm^{-1}, E = 0.4 cm^{-1}, $g_x = g_y$ = 2.43, and g_z = 2.25. The results are compatible with the easy-plane magnetic anisotropy with a large positive D value. We have also obtained the set of fit results with the parameters D = -12.1 cm^{-1}, E = 11.5 cm^{-1}, $g_x = g_y$ = 2.31, and g_z = 2.49. However, the negative anisotropy conflicts with the theoretical results. Furthermore, the positive D values occurred in the reported Co(II) compounds with pentagonal bipyramidal geometry (D_{5h} symmetry).

As a Kramers ion, the Co(II) complexes frequently showed slow magnetic relaxation behaviour, characteristic of a single-ion magnet. Firstly, ac magnetic susceptibility measurements were performed under

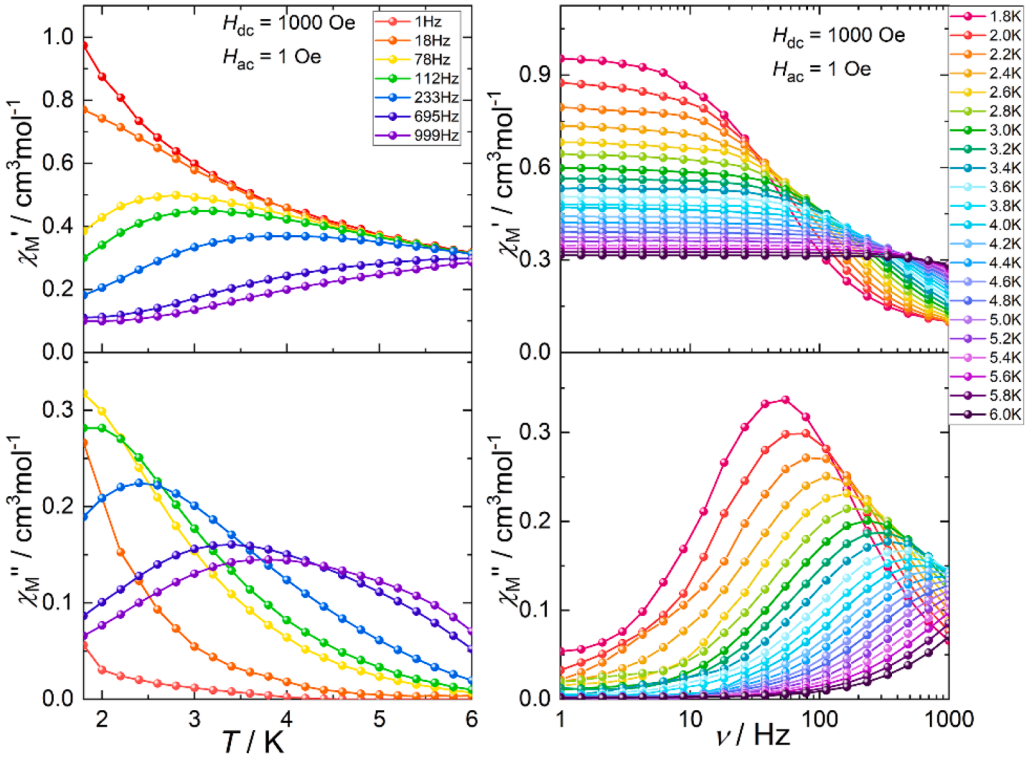

Fig. 3. Temperature dependence and Frequency dependence of the in-phase (χ_M') and out-of-phase (χ_M'') parts of the ac susceptibility for complex **1** in the range of 1.8–6.0 K and 1 Hz −999 Hz under a 1000 Oe dc field.

zero applied dc field, (Fig. S1) and no out-of-phase ac susceptibility was observed for complex **1**, probably resulting from the fast QTM for the most mononuclear Co(II) SMMs. To suppress the fast QTM relaxation effects for **1**, ac susceptibility measurements at 2 K under various dc bias fields (200–4000 Oe) were performed to give the optimistic dc field 1000 Oe. As shown in Fig. 3, the temperature-dependent and frequency-dependent ac susceptibility curves identified the slow magnetic relaxation behavior of complex **1**. To evaluate the dynamic magnetic parameters, the Cole-Cole plots can be fitted well by using the generalized Debye model [37] (Fig. 4a), which exhibited semicircle shapes extracting the data from the ac susceptibilities. The parameter α values are in the range of 0.05 to 0.19 (see Table S2), suggesting a substantial broadening of the distribution of magnetic relaxation times, especially at low temperatures. The Arrhenius law $\tau^{-1} = \tau_0^{-1}\exp(-U_{eff}/k_BT)$ can be applied for the fit of the high-temperature data (T = 5.0–6.0 K, Fig. 4b) to obtain the effective energy barrier (U_{eff}). The results gave U_{eff} = 29.5 K and $\tau_0 = 4.0 \times 10^{-7}$ s. However, the curvature of the plots indicates the existence of multiple relaxation pathways. Because of the applied dc field, the multiple relaxation processes can be regarded as the spin–lattice relaxation with Raman and Orbach processes ($\tau^{-1} = CT^n + \tau_0^{-1}\exp(-U_{eff}/k_BT)$. The best fit in the whole temperature region (Fig. 4b) yields the parameters C = 53.9 $K^{-3.0}$ s^{-1}, n = 3.0, U_{eff} = 55.9 K and $\tau_0 = 2.2 \times 10^{-10}$ s. The observed energy barrier is larger than the barrier only considering the Orbach process, and the obtained n value is consistent with the optical acoustic Raman process [38].

3.3. Theoretical calculations of complex *1*

To estimate the zero-field splitting parameter in **1**, here we have performed complete active space self-consistent field (CASSCF) [31] followed by second-order *N*-electron valence perturbation theory (NEVPT2) [32–34] on the hydrogen optimized X-ray crystal structure (see ESI for the details). CASSCF/NEVPT2 methodology has been instrumental in computing the spin-Hamiltonian (SH) parameters of open-shell transition metal complexes [39–43]. In complex **1**, the Co(II) is seven-coordinated, possessing a distorted pentagonal bipyramidal environment, where -NCS ligands are present on the axial position while pypzbeyz ligand and DMF are present in the plane. NEVPT2 computed all the ten quartet states (^{4}F and ^{4}P) spanned over an energy range of ~ 24050 cm^{-1}, with the first excited spin-free state located at ~ 2222 cm^{-1} higher in energy. In a perfect D_{5h} environment, the ^{4}F state splits in the $4A_2' + 4E_2'' + 4E_1'' + 4E_2'$ states, and due to structural distortions, we have observed the non-degenerate $4A_2'$ as the ground state while excited $4E_2'' + 4E_1'' + 4E_2'$ states(See Fig. 5(a)). NEVPT2-AILFT predicts the following orbital ordering $(d_{xz})^2 < (d_{yz})^2 < (d_{x2-y2})^1 < (d_{xy})^1 < (d_{z2})^1$, representing the distorted Co(II) ion in the PBP environment (See Fig. 5 (b)) [17,44–46]. CASSCF/NEVPT2 computed spin-free and spin–orbit states are reported in Table S3. NEVPT2(CASSCF) computed energy gap between the ground and first excited Kramer Doublet (K_D) is 67.4 (77.0) cm^{-1}. Wave functional decomposition analysis of the ground and first excited state KDs are 60 % $|3/2; \pm1/2\rangle$ + 36 % $|3/2; \pm3/2\rangle$and 65 % $|3/2; \pm3/2\rangle$ + 31 % $|3/2; \pm1/2\rangle$. The projection of the quartet and doublet excited states of the NEVPT2(CASSCF) calculations on S = 3/2 pseudo-spin yields a D value of 33.5 (38.2) cm^{-1} for complex **1**. NEVPT2 (CASSCF) computed E/D values are 0.06(0.07) very small. The computed D and E values are in good agreement with the experiment. NEVPT2 computed g-values for the ground state K_D of **1** are g_{min} = 2.032; g_{mid} = 4.260 and g_{max} = 5.191 representing significantly large transverse anisotropy, which is in line with the experimentally observed easy plane anisotropy (see Table S4 for details). The computed D-tensor orientation is provided in Fig. S3. Our calculations nicely reproduce the experimental static dc data, highlighting the correctness of the computed SH parameters.

Generally, the Co(II) PBP complexes possess a mild positive D value within the range of ~20–60 cm^{-1} [17,44–52]. In the D_{5h} environment, the non-degenerate $4A_2'$ becomes the ground state, and magnetic anisotropy emerges from the second-order SOC via mixing with the excited states [44–49]. The large crystal field splitting due to the seven coordinating ligands throws the first spin-free excited state higher in energy, hence limiting the magnitude of the zero-field splitting parameters. NEVPT2 computed the first excited spin-free state located at ~2222 cm^{-1} for **1**. For complex **1**, the ground configuration is 81 % $(d_{xy})^1(d_{yz})^2(d_{z^2})^1(d_{xz})^2(d_{x^2-y^2})^1$ and the first excited state configuration is 51 % $(d_{xy})^1(d_{yz})^1(d_{z^2})^1(d_{xz})^2(d_{x^2-y^2})^2$ + 18 % $(d_{xy})^2(d_{yz})^1(d_{z^2})^1(d_{xz})^2(d_{x^2-y^2})^1$. It is evident from the nature of the first excited configuration that the major contribution to the D value emerges from $d_{yz}\rightarrow d_{x2-y2}$ transition (i.e. between different $|m_l|$ levels), which explains the positive zero-field splitting in **1**. Moreover, small contributions from the spin-flip excitations to D values have also been witnessed (see Table S5 and S6 for details). The spin-conserved excitations are the major contributors to the D value and due to doubly occupied d_{xz}/d_{yz} orbitals, the spin-conserved transition only takes place between the orbitals of the different m_l levels and ensures the positive D value for Co(II) PBP complexes. To conclude, the axial ligand donor strength and the equatorial ligand symmetry affect the sign and magnitude of D. In complex **1**, the axial ligands are weak σ-donors and the equatorial ligand is asymmetric, which caused the spin–orbit mixing of the ground quartet with the excited quartet level to give the positive D value for the Co(II)

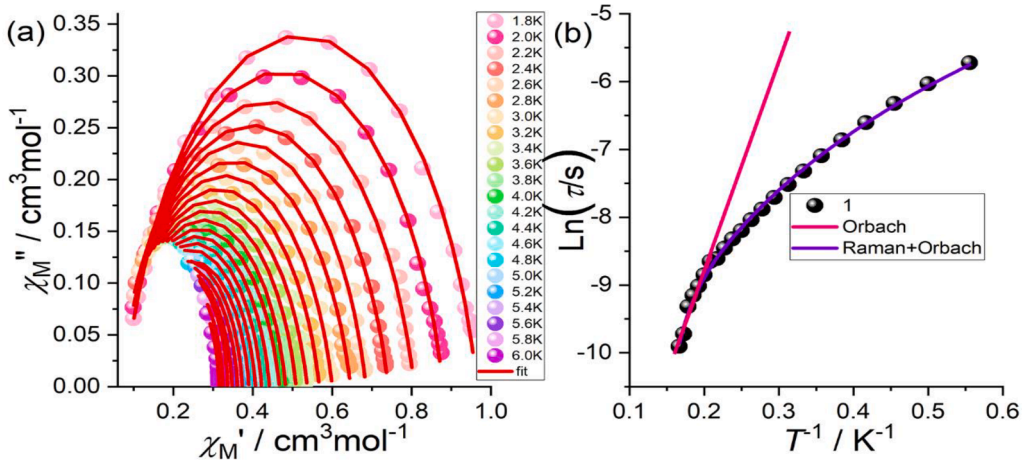

Fig. 4. (a) Cole-Cole plots of **1** measured under 1000 Oe dc field from 1.8 to 6.0 K. The red solid lines correspond to the best fit obtained with a generalized Debye model. (b) The relaxation time of the magnetization ln(τ) vs T^{-1} for **1**. The pink line corresponds to the Arrhenius fit in the high range of 5.0–6.0 K and the violet line corresponds to the fit using Raman and Orbach processes. ((Colour online.))

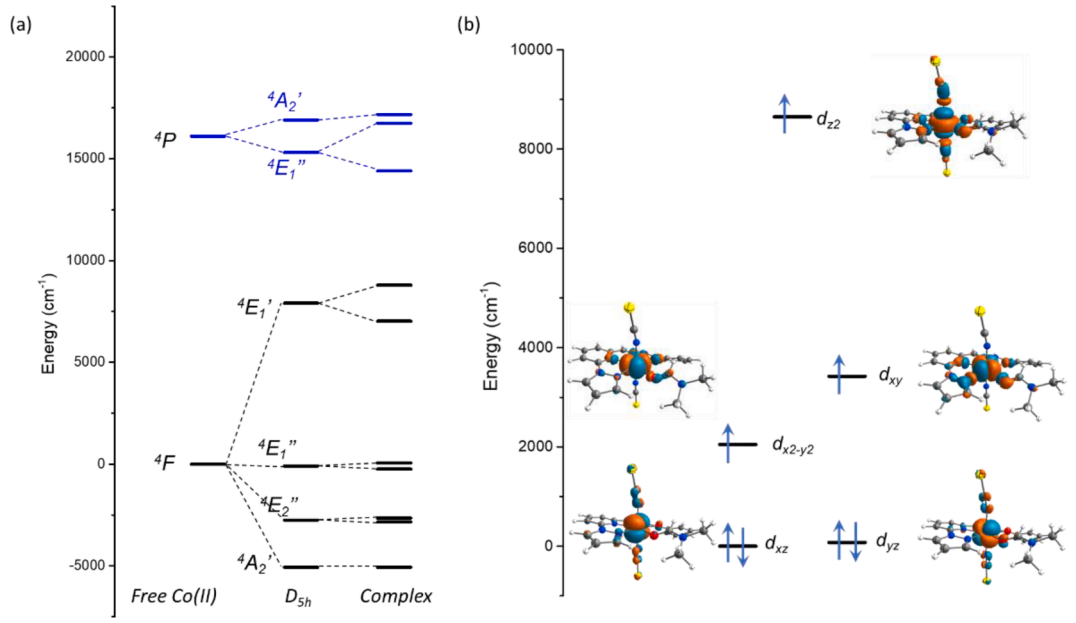

Fig. 5. (a) NEVPT2 computed energy splitting diagram of free Co(II) in ideal D_{5h} environment complex **1** (b) NEVPT2-Ab-initio ligand field theory (AILFT) computed *d*-orbital ordering for **1**.

complex with pentagonal bipyramidal geometry [18,53].

4. Conclusions

In conclusion, a Co(II) complex based on an asymmetric tetradentate ligand has been synthesized and characterized. The Co(II) complex is seven-coordinate with pentagonal bipyramidal geometry (D_{5h} symmetry). Magnetic measurements revealed that the high-spin Co(II) complex possesses an easy-plane magnetic anisotropy with a positive *D* value and a small *E* value. Additionally, the high-coordinate Co(II) complex exhibited a field-induced SIM behavior. Furthermore, the results obtained from CASSCF/NEVPT2 calculations in the Co(II) complex display large easy plane anisotropy and agree with the experimental findings. Further efforts include designing and constructing the high-coordinate 3d SIMs with a ligand design strategy.

CRediT authorship contribution statement

Xing-Cai Huang: Supervision, Conceptualization, Writing – original draft, Funding acquisition. **Wei Yong:** Methodology, Data curation. **Shruti Moorthy:** Data curation, Software. **Zhang-Yu Su:** Methodology, Data curation, Validation. **Jiao-Jiao Kong:** Writing – review & editing. **Saurabh Kumar Singh:** Writing – review & editing, Funding acquisition.

Declaration of Competing Interest

The authors declare that they have no known competing financial interests or personal relationships that could have appeared to influence the work reported in this paper.

Data availability

Data will be made available on request.

Acknowledgments

This research was supported by the National Natural Science Foundation of China (grant No. 21601153), the Qing-Lan Project of Jiangsu Province (X-C. Huang), and State Key Laboratory of Coordination Chemistry, Nanjing University (SKLCC2105). SKS thanks IIT Hyderabad and Start-up Research Grant (SRG/2020/001323) from Department of Science and Technology. SM thanks PMRF Fellowship. SKS and SM acknowledges PARAM Seva Computing Facility under the National Supercomputing Mission, at IIT Hyderabad.

Appendix A. Supplementary data

CCDC 2217639 contains the supplementary crystallographic data for complex **1**. These data can be obtained free of charge via https://www.ccdc.cam.ac.uk/conts/retrieving.html, or from the Cambridge Crystallographic Data Centre, 12 Union Road, Cambridge CB2 1EZ, UK; fax: (+44) 1223–336-033; or e-mail: deposit@ccdc.cam.ac.uk. Supplementary data to this article can be found online at https://doi.org/10.1016/j.poly.2022.116275.

References

[1] E. Coronado, Molecular magnetism: from chemical design to spin control in molecules, materials and devices, Nat. Rev. Mater. 5 (2020) 87–104.
[2] M.N. Leuenberger, D. Loss, Quantum computing in molecular magnets, Nature 410 (2001) 789–793.
[3] E. Moreno-Pineda, W. Wernsdorfer, Measuring molecular magnets for quantum technologies, Nat. Rev. Phys. 3 (2021) 645–659.
[4] S.L. Bayliss, D.W. Laorenza, P.J. Mintun, B.D. Kovos, D.E. Freedman, D. D. Awschalom, Optically addressable molecular spins for quantum information processing, Science 370 (2020) 1309–1312.
[5] L. Bogani, W. Wernsdorfer, Molecular spintronics using single-molecule magnets, Nat. Mater. 7 (2008) 179–186.
[6] D.E. Freedman, W.H. Harman, T.D. Harris, G.J. Long, C.J. Chang, J.R. Long, Slow Magnetic Relaxation in a High-Spin Iron(II) Complex, J. Am. Chem. Soc. 132 (2010) 1224–1225.
[7] P.C. Bunting, M. Atanasov, E. Damgaard-Møller, M. Perfetti, I. Crassee, M. Orlita, J. Overgaard, J. van Slageren, F. Neese, J.R. Long, A linear cobalt(II) complex with maximal orbital angular momentum from a non-Aufbau ground state, Science, 362 (2018) eaat7319.
[8] J.M. Zadrozny, J. Liu, N.A. Piro, C.J. Chang, S. Hill, J.R. Long, Slow magnetic relaxation in a pseudotetrahedral cobalt(ii) complex with easy-plane anisotropy, Chem. Commun. 48 (2012) 3927–3929.
[9] P.P. Samuel, K.C. Mondal, N. Amin Sk, H.W. Roesky, E. Carl, R. Neufeld, D. Stalke, S. Demeshko, F. Meyer, L. Ungur, L.F. Chibotaru, J. Christian, V. Ramachandran, J. van Tol, N.S. Dalal, Electronic structure and slow magnetic relaxation of low-coordinate cyclic alkyl(amino) carbene stabilized iron(I) complexes, J. Am. Chem. Soc. 136 (2014) 11964–11971.
[10] M.R. Saber, K.R. Dunbar, Ligands effects on the magnetic anisotropy of tetrahedral cobalt complexes, Chem. Commun. 50 (2014) 12266–12269.

[11] S. Vaidya, A. Upadhyay, S.K. Singh, T. Gupta, S. Tewary, S.K. Langley, J.P. S. Walsh, K.S. Murray, G. Rajaraman, M. Shanmugam, A synthetic strategy for switching the single ion anisotropy in tetrahedral Co(ii) complexes, Chem. Commun. 51 (2015) 3739–3742.
[12] C. Rajnák, J. Titiš, O. Fuhr, M. Ruben, R. Boča, Single-molecule magnetism in a pentacoordinate cobalt(II) complex supported by an antenna ligand, Inorg. Chem. 53 (2014) 8200–8202.
[13] N. Nedelko, A. Kornowicz, I. Justyniak, P. Aleshkevych, D. Prochowicz, P. Krupiński, O. Dorosh, A. Ślawska-Waniewska, J. Lewiński, Supramolecular control over molecular magnetic materials: γ-cyclodextrin-templated grid of cobalt (II) single-ion magnets, Inorg. Chem. 53 (2014) 12870–12876.
[14] E. Colacio, J. Ruiz, E. Ruiz, E. Cremades, J. Krzystek, S. Carretta, J. Cano, T. Guidi, W. Wernsdorfer, E.K. Brechin, Slow magnetic relaxation in a CoII–YIII single-ion magnet with positive axial zero-field splitting, Angew. Chem. Int. Ed. 52 (2013) 9130–9134.
[15] J. Vallejo, I. Castro, R. Ruiz-García, J. Cano, M. Julve, F. Lloret, G. De Munno, W. Wernsdorfer, E. Pardo, Field-induced slow magnetic relaxation in a six-coordinate mononuclear cobalt(II) complex with a positive anisotropy, J. Am. Chem. Soc. 134 (2012) 15704–15707.
[16] J. Vallejo, M. Viciano-Chumillas, F. Lloret, M. Julve, I. Castro, J. Krzystek, M. Ozerov, D. Armentano, G. De Munno, J. Cano, Coligand effects on the field-induced double slow magnetic relaxation in six-coordinate cobalt(II) single-ion magnets (SIMs) with positive magnetic anisotropy, Inorg. Chem. 58 (2019) 15726–15740.
[17] X.-C. Huang, C. Zhou, D. Shao, X.-Y. Wang, Field-induced slow magnetic relaxation in cobalt(II) compounds with pentagonal bipyramid geometry, Inorg. Chem. 53 (2014) 12671–12673.
[18] A.K. Mondal, A. Mondal, B. Dey, S. Konar, Influence of the coordination environment on easy-plane magnetic anisotropy of pentagonal bipyramidal cobalt (II) complexes, Inorg. Chem. 57 (2018) 9999–10008.
[19] M. Peng, X.-F. Wu, L.-X. Wang, S.-H. Chen, J. Xiang, X.-X. Jin, S.-M. Yiu, B.-W. Wang, S. Gao, T.-C. Lau, Slow magnetic relaxation in high-coordinate Co(ii) and Fe(ii) compounds bearing neutral tetradentate ligands, Dalton Trans. 50 (2021) 15327–15335.
[20] D. Shao, S.-L. Zhang, L. Shi, Y.-Q. Zhang, X.-Y. Wang, Probing the effect of axial ligands on easy-plane anisotropy of pentagonal-bipyramidal cobalt(II) single-ion magnets, Inorg. Chem. 55 (2016) 10859–10869.
[21] X.-C. Huang, R. Xu, Y.-Z. Chen, Y.-Q. Zhang, D. Shao, Two four-coordinate and seven-coordinate CoII complexes based on the bidentate ligand 1, 8-naphthyridine showing slow magnetic relaxation behavior, Chemistry 15 (2020) 279–286.
[22] X.-C. Huang, Z.-Y. Qi, C.-L. Ji, Y.-M. Guo, S.-C. Yan, Y.-Q. Zhang, D. Shao, X.-Y. Wang, High-coordinate CoII and FeII compounds constructed from an asymmetric tetradentate ligand show slow magnetic relaxation behavior, Dalton Trans. 47 (2018) 8940–8948.
[23] O. Kahn, Molecular Magnetism, in, VCH publishers Inc., 1993.
[24] SAINT, in, Bruker AXS, Inc., Madison, WI, 2009.
[25] L. Krause, R. Herbst-Irmer, G.M. Sheldrick, D. Stalke, Comparison of silver and molybdenum microfocus X-ray sources for single-crystal structure determination, J Appl Crystallogr 48 (2015) 3–10.
[26] G.M. Sheldrick, Crystal structure refinement with SHELXL, Acta Crystallographica Section C, Struct. Chem. 71 (2015) 3–8.
[27] F. Neese, Software update: the ORCA program system, version 4.0, WIREs Computational Molecular, Science 8 (2018) e1327.
[28] J.P. Perdew, Density-functional approximation for the correlation energy of the inhomogeneous electron gas, Phys. Rev. B 33 (1986) 8822–8824.
[29] A.D. Becke, Density-functional exchange-energy approximation with correct asymptotic behavior, Phys. Rev. A 38 (1988) 3098–3100.
[30] F. Weigend, R. Ahlrichs, Balanced basis sets of split valence, triple zeta valence and quadruple zeta valence quality for H to Rn: Design and assessment of accuracy, PCCP 7 (2005) 3297–3305.
[31] P.-Å. Malmqvist, B.O. Roos, The CASSCF state interaction method, Chem. Phys. Lett. 155 (1989) 189–194.
[32] C. Angeli, R. Cimiraglia, S. Evangelisti, T. Leininger, J.P. Malrieu, Introduction of n-electron valence states for multireference perturbation theory, J. Chem. Phys. 114 (2001) 10252–10264.
[33] C. Angeli, R. Cimiraglia, J.-P. Malrieu, N-electron valence state perturbation theory: a fast implementation of the strongly contracted variant, Chem. Phys. Lett. 350 (2001) 297–305.
[34] C. Angeli, R. Cimiraglia, J.-P. Malrieu, n-electron valence state perturbation theory: A spinless formulation and an efficient implementation of the strongly contracted and of the partially contracted variants, J. Chem. Phys. 117 (2002) 9138–9153.
[35] V. Shape, in: D.C. Miquel Llunell, Jordi Cirera, Pere Alemany and Santiago Alvarez (Ed.), Universitat de Barcelona, 2013.
[36] N.F. Chilton, R.P. Anderson, L.D. Turner, A. Soncini, K.S. Murray, PHI: A powerful new program for the analysis of anisotropic monomeric and exchange-coupled polynuclear d- and f-block complexes, J. Comput. Chem. 34 (2013) 1164–1175.
[37] K.S. Cole, R.H. Cole, Dispersion and absorption in dielectrics I. alternating current characteristics, J. Chem. Phys. 9 (1941) 341–351.
[38] K.N. Shrivastava, Theory of spin-lattice relaxation, Phys. Status Solidi (b) 117 (1983) 437–458.
[39] S. Gómez-Coca, A. Urtizberea, E. Cremades, P.J. Alonso, A. Camón, E. Ruiz, F. Luis, Origin of slow magnetic relaxation in Kramers ions with non-uniaxial anisotropy, Nat. Commun. 5 (2014) 4300.
[40] D.H. Moseley, S.E. Stavretis, K. Thirunavukkuarasu, M. Ozerov, Y. Cheng, L. L. Daemen, J. Ludwig, Z. Lu, D. Smirnov, C.M. Brown, A. Pandey, A.J. Ramirez-Cuesta, A.C. Lamb, M. Atanasov, E. Bill, F. Neese, Z.-L. Xue, Spin–phonon couplings in transition metal complexes with slow magnetic relaxation, Nat. Commun. 9 (2018) 2572.
[41] D. Shao, S. Moorthy, X. Yang, J. Yang, L. Shi, S.K. Singh, Z. Tian, Tuning the structure and magnetic properties via distinct pyridine derivatives in cobalt(ii) coordination polymers, Dalton Trans. 51 (2022) 695–704.
[42] D. Shao, S. Moorthy, Y. Zhou, S.-T. Wu, J.-Y. Zhu, J. Yang, D.-Q. Wu, Z. Tian, S. K. Singh, Field-induced slow magnetic relaxation behaviours in binuclear cobalt(ii) metallocycles and exchange-coupled clusters, Dalton Trans. 51 (2022) 9357–9368.
[43] Z. Tian, S. Moorthy, H. Xiang, P. Peng, M. You, Q. Zhang, S.-Y. Yang, Y.-L. Zhang, D.-Q. Wu, S.K. Singh, D. Shao, Tuning chain topologies and magnetic anisotropy in one-dimensional cobalt(ii) coordination polymers via distinct dicarboxylates, CrstEngComm 24 (2022) 3928–3937.
[44] F. Schleife, A. Rodenstein, R. Kirmse, B. Kersting, Seven-coordinate Mn(II) and Co (II) complexes of the pentadentate ligand 2,6-diacetyl-4-carboxymethyl-pyridine bis(benzoylhydrazone): Synthesis, crystal structure and magnetic properties, Inorg. Chim. Acta 374 (2011) 521–527.
[45] R. Ruamps, L.J. Batchelor, R. Maurice, N. Gogoi, P. Jiménez-Lozano, N. Guihéry, C. de Graaf, A.-L. Barra, J.-P. Sutter, T. Mallah, Origin of the magnetic anisotropy in heptacoordinate NiII and CoII complexes, Chem. – A Eur. J. 19 (2013) 950–956.
[46] M. Dey, S. Dutta, B. Sarma, R.C. Deka, N. Gogoi, Modulation of the coordination environment: a convenient approach to tailor magnetic anisotropy in seven coordinate Co(ii) complexes, Chem. Commun. 52 (2016) 753–756.
[47] B. Drahoš, R. Herchel, Z. Trávníček, Structural, magnetic, and redox diversity of first-row transition metal complexes of a pyridine-based macrocycle: well-marked trends supported by theoretical DFT calculations, Inorg. Chem. 54 (2015) 3352–3369.
[48] B. Drahos, I. Cisarova, O. Laguta, V.T. Santana, P. Neugebauer, R. Herchel, Structural, magnetic, redox and theoretical characterization of seven-coordinate first-row transition metal complexes with a macrocyclic ligand containing two benzimidazolyl N-pendant arms, Dalton Trans. 49 (2020) 4425–4440.
[49] G. Yi, C. Zhang, W. Zhao, H. Cui, L. Chen, Z. Wang, X.-T. Chen, A. Yuan, Y.-Z. Liu, Z.-W. Ouyang, Structure, magnetic anisotropy and relaxation behavior of seven-coordinate Co(ii) single-ion magnets perturbed by counter-anions, Dalton Trans. 49 (2020) 7620–7627.
[50] P. Comba, G. Rajaraman, A. Sarkar, G. Velmurugan, What controls the magnetic anisotropy in heptacoordinate high-spin cobalt(ii) complexes? A theoretical perspective, Dalton Trans. 51 (2022) 5175–5183.
[51] L. Vaiana, M. Regueiro-Figueroa, M. Mato-Iglesias, C. Platas-Iglesias, D. Esteban-Gómez, A. de Blas, T. Rodríguez-Blas, Seven-coordination versus six-coordination in divalent first-row transition-metal complexes derived from 1,10-Diaza-15-crown-5, Inorg. Chem. 46 (2007) 8271–8282.
[52] L. Chen, S.-Y. Chen, Y.-C. Sun, Y.-M. Guo, L. Yu, X.-T. Chen, Z. Wang, Z.W. Ouyang, Y. Song, Z.-L. Xue, Slow magnetic relaxation in mononuclear seven-coordinate cobalt(ii) complexes with easy plane anisotropy, Dalton Trans. 44 (2015) 11482–11490.
[53] A. Sarkar, S. Dey, G. Rajaraman, Role of coordination number and geometry in controlling the magnetic anisotropy in Fe(II), Co(II), and Ni(II) single-ion magnets,, Chemistry – A Eur. J. 26 (2020) 14036–14058.